Jurnal Teknologi

Full Paper

EVALUATION OF THE EDGE PROFILE SHIFTING BASED ON STATISTICAL APPROACH TO IMPROVE THE EDGE-BASED MTF MEASUREMENT

Riska Amilia[a], Choirul Anam[a]*, Karrar Mahdi Badi[b], Ariij Naufal[a], Geoff Dougherty[c]

[a]Department of Physics, Faculty of Sciences and Mathematics, Diponegoro University, Jl. Prof. Soedarto SH, Tembalang, Semarang 50275, Central Java, Indonesia
[b]Department of Medical Physics, College of Science, Al-Qadisiyah University, Al-Qadisiyah, Iraq
[c]Applied Physics and Medical Imaging, California State University Channel Islands, Camarillo, CA 93012, USA

Article history
Received
3 April 2024
Received in revised form
27 July 2024
Accepted
26 August 2024
Published Online
28 April 2025

*Corresponding author
anam@fisika.fsm.undip.ac.id

Graphical abstract

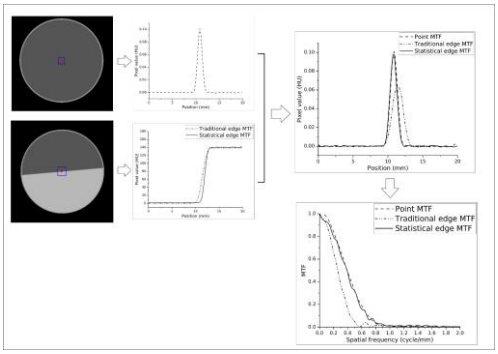

Abstract

This study aims to evaluate the accuracy of edge profile shifting based on a statistical approach to improve the edge-based modulation transfer function (MTF) measurement using the slanted-edge phantom. A slanted-edge phantom was computationally developed with two materials, a water and a material of 120 HU. The spatial resolution of the phantom was varied from 0.3 to 1.25 cycle/mm and the slanted angle was varied from 0° to 10°. The statistical shifting was performed by shifting the treated ESF backward and forward by up to 10 pixels (increment of 1 pixel). At each shift, the similarity between the shifted and reference ESFs was calculated using mean squared error (MSE). The statistical edge-MTF was compared against the traditional edge-MTF and the point-MTF as the gold standard. The statistical edge-MTF approach had similar results against the point-MTF compared to the traditional edge-MTF. At a slanted angle less than 8°, the statistical edge-MTF was comparable to the point-MTF with a difference about 2%. For slanted angles more than 8°, the difference was around 5%. By contrast, the non-statistical edge-MTF approach produced larger differences as the slanted angle increased. The statistical approach for measuring edge-MTF is more robust compared to the traditional edge-MTF approach.

Keywords: Computed Tomography, modulation transfer function, slanted edge method, spatial resolution

1.0 INTRODUCTION

Spatial resolution defines a scanner's ability to portray the fine detail of an object within an image [1]. This parameter is used to assess whether two small objects can still be recognized as two separate objects in an image [2-3]. Measuring the spatial resolution is usually carried out by visualizing the number of line pairs or hole pairs per millimeter. If a higher number of resolvable objects is visualized, then the image has a higher spatial resolution [4-5]. However, this method is subjective so an advanced approach to objectively measure spatial resolution was introduced using the modulation transfer function (MTF) [2, 6, 7].

The MTF can be assessed by employing the point spread function (PSF), i.e., the distribution of pixel values in the image of a point object. The PSF depicts the unsharpness of the image of a point object. Since the PSF describes the transfer of a two-dimensional (2D) object, the 2D PSF is commonly averaged to find the 1D PSF to more conveniently characterize the broadening of an object [6]. Calculating the MTF is usually carried out by taking the Fourier transform of the 1D PSF curve [6, 8-10].

Another method to determine the MTF is by using the edge spread function (ESF) [11-12]. The ESF has an advantage over the PSF because more spread profiles are obtained which can then be averaged to minimize impact of the image noise on the resulted MTF [13]. ESFs are taken at the edge of an object within an image. To obtain adequate sampling from the edge object within the clinical field of view (FOV), one of the commonly used techniques is to employ the slanted-edge method [14-17]. The profiles of the edge images are then carefully re-binned and shifted so that an adequate sampling of the edge profile is obtained [18-20]. To achieve this goal, the slight angle of the linear slanted-edge should be known [21]. Therefore, it cannot be carried out if the angle of the linear slanted-edge is not known or if the edge is not linear (i.e. such as an irregular edge in an anthropomorphic phantom or patient). It is noted that efforts to obtain the MTF from a clinical image of a patient is an ongoing process [22].

It is already mentioned that obtaining an accurate ESF is dependent on the accurate shifting of the ESF [19]. To achieve the accurate shifting from a linear slanted-edge, the angle of the slanted-edge should be employed and the fit of the curves should be carefully implemented. Previous studies from numerous researchers (i.e., Zhang *et al*. [16], Zhou *et al*. [19], Yuan *et al*. [23] and Mori *et al*. [24]) have investigated the accuracy of this method. However, implementing an accurate edge detection requires a complicated calculation and is time consuming [16]. A simpler method to accurately shift the ESF is desirable.

To overcome this challenge, a novel but simple method for accurate shifting of the ESF based on statistics is proposed. In this method, there is one reference ESF and the other ESFs are shifted forward and backward a few pixels. The ESF at a certain position (which is statistically closest to the reference ESF) is determined as the best shifting. The advantage of this method is that it can be applied not only to linear slanted-edges, but also to all types of edges (including irregular edges, such as in anthropomorphic phantoms or patients). In addition, a fitting is not needed for this method. In this paper, the accuracy of this method is evaluated on images of linear slanted-edges with varying spatial resolution and varying angles.

2.0 METHODOLOGY

2.1 Computational phantom

Software for developing the computational phantom has been developed previously [25-27]. A modification of the previous phantom (512 × 512 pixels with a field-of-view (FOV) of 250 mm) was carried out in this study. The background of the phantom was air with a CT number of -1000 HU. The phantom's case was acrylic with a CT number of 120 HU. The outer diameter (d_1) was 200 mm and inner diameter (d_2) was 98% of outer diameter (d_2 = 98% d_1). Within the phantom, there were two semi-circular objects. One object had a CT number of 0 HU and the other had a CT number of 140 HU. The angle of inclination of their borders can be adjusted. In this study, the slanted-edge was set from 0° to 10° with 1° increments. An example of phantom images with varying slanted angles from 0° to 10° with 2° increments is shown in Figure 1.

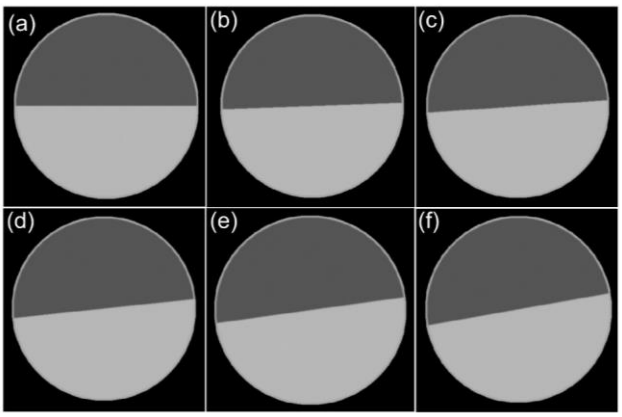

Figure 1 The development of the slanted-edge computational phantom with various angles: (a) 0°, (b) 2°, (c) 4°, (d) 6°, (e) 8°, and (f) 10°

In order to mimick an actual CT image (*I(x, y)*), a certain level of spatial resolution of the phantom was achieved by convolving the original image (*P(x, y)*) with a 2-dimensional point spread function (*PSF(x, y)*) having matric size of 15 x 15 pixels and addition the Gaussian noise (*N(x, y)*) of 1 HU (Equation 1).

$$I(x,y) = \frac{1}{k}[P(x,y) \otimes PSF(x,y)] + N(x,y) \quad (1)$$

The Gaussian point spread function was computed using Equation (2):

$$PSF(x,y) = e^{-\left(\frac{x^2+y^2}{2\sigma^2}\right)} \quad (2)$$

where σ is the standard deviation (SD) of the function and it indicates amount of blur. In this study, σ was varied from 0.5 to 2.1 pixels with increments of 0.2 pixels to obtain spatial resolution from 0.3 to 1.25 cycle/mm.

In the convolution process, normalization was carried out using *k* factor which is formulated by Equation (3).

$$k = \sum\sum(PSF(x,y)) \quad (3)$$

The phantom *I(x, y)* was then ready to be used in an evaluation of edge profile shifting based on a statistical approach to improve the edge-based MTF measurement.

2.2 MTF Measurement

The MTF measurement was performed based on the PSF and ESF edges of the slanted object. The ESFs were used both unshifted and shifted using a statistical approach. The statistical approach is expected to give a more accurate MTF. Automated MTF measurement using the unshifted edge has been previously developed on a PMMA phantom and has a difference of about 4% from the point MTF [26]. In this paper, the MTF from the shifted ESFs using a statistical approach is called the statistical edge-MTF, the MTF from the unshifted ESF is called the traditional edge-MTF, and the MTF from a point object is called the point-MTF.

The schematic diagram of the current study is shown in Figure 2.

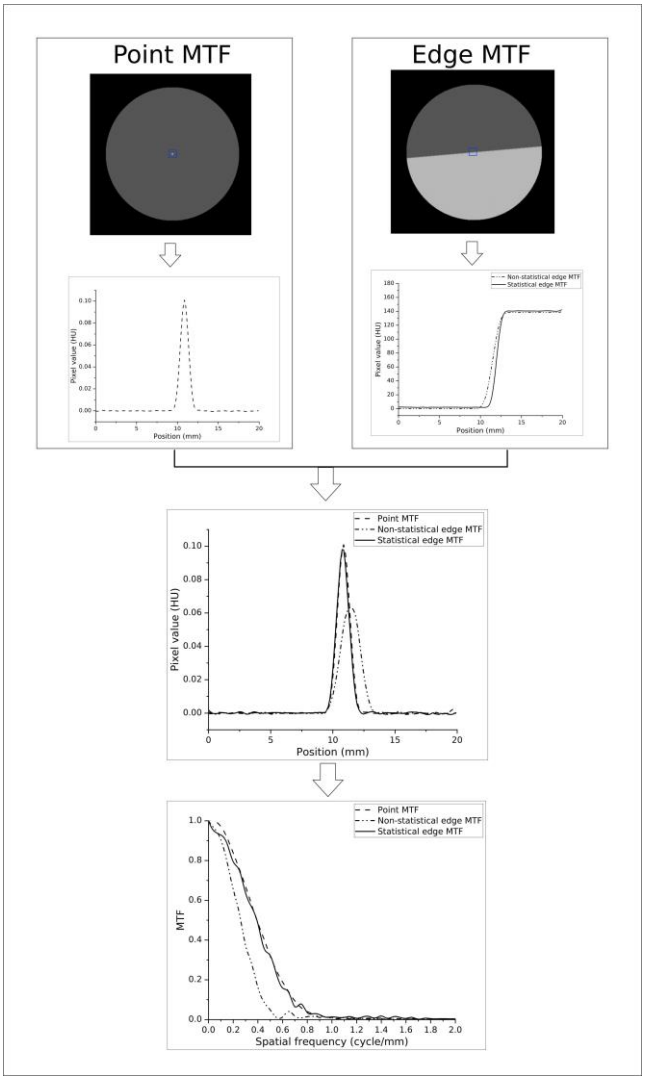

Figure 2 The schematic diagram of the current study. Point-MTF is considered to be the gold standard. Edge-MTF is performed with two approaches, i.e. with and without statistical shifting of their ESFs

The point-MTF is considered the gold-standard in this study. Measuring the point-MTF utilized the point-computational phantom [29]. A region of interest (ROI) of size 32 × 32 pixels was placed at the centroid of the phantom. The profile of CT numbers in the x-axis was obtained by averaging the pixels along the *y*-direction (*S(x)*). Next, the profile of CT number was zeroed (*S'(x)*) and normalized to obtain the 1D *PSF(x)* curve using Equation (4). The 1D *PSF(x)* curve was Fourier transformed using Equation (5) to obtain the *MTF(f)* curve, where *F* is the Fourier operator and *f* is the spatial frequency.

$$PSF\ (x) = \frac{S'(x)}{\sum_{i=1}^{n} S'(x_i)} \quad (4)$$

$$MTF(f) = \mathcal{F}\big(PSF(x)\big) = \int_{-\infty}^{+\infty} \big[PSF(x)e^{-2\pi jxf}\big]dx \quad (5)$$

The edge-MTF measurement on the slanted edge phantom was started by placing a square-shaped ROI of 20 × 20 pixels at the centroid of the phantom as in Figure 2. As a result, the profile of the CT number along the *y*-axis can be obtained and was presented as an ESF curve.

For the traditional edge-MTF, the measurement process was performed using a previous algorithm [29] and is shown in Figure 2. The ESF curves were averaged to obtain a single ESF. The ESF curve was differentiated to obtain the PSF curve which was Fourier transformed as before to obtain the edge-MTF.

In the statistical edge-MTF, the ESF curve is pre-processed. The alignment of the ESF phase was performed on two ESFs. A middle ESF was considered the reference ESF and the other ESFs were considered the treated ESFs. The treated ESFs were shifted one by one using a statistical approach. One of the treated ESFs was shifted 20 times. It was shifted by 10 pixels in steps of 1 pixel to the left, and shifted by 10 pixels in steps of 1 pixel to the right. To maintain the length of the treated ESF, the deleted pixels at one end of the profile were compensated by adding pixels at the other end of the profile. At each shift of one pixel, the level of difference (or similarity) between the shifted and reference ESFs was measured using the mean square error (MSE) (Equation 6). The optimal shift position was the shift that produce a minimum MSE.

$$MSE = \frac{1}{N}\sum_{i=1}^{N}(x_i - y_i)^2 \quad (6)$$

This process was a shifting for a single treated ESF. For shifting all treated ESFs, the process was iterated for the remaining ESF samples. The results of shifted ESFs were averaged to obtain a single ESF curve. The resulting ESF curve was used to obtain the statistical edge-MTF using the same steps as before.

The independent sample *t*-test was conducted to investigate whether there was a significant difference between the 10% levels of the respective edge-MTFs (traditional and statistical edge-MTFs) and the point-MTF. The calculation was employed by using IBM SPSS

Statistics 25. If the test produced a *p*-value greater than 0.05, the methods did not differ significantly.

3.0 RESULTS AND DISCUSSION

3.1 Spatial Resolution Variation

The point-MTF, the traditional edge-MTF, and the statistical edge-MTF curves at various spatial resolutions are shown in Figure 3 and their values of MTF 10% are tabulated in Table 1. It is noted that the angle of the slanted image for edge-MTF is 5°. The statistical edge-MTFs produce values that are close (within 1-2 %) to the point-MTFs at medium spatial resolutions of 0.9 – 1.9 cycle/mm. However, at high and low spatial resolutions, the results obtained between both methods were quite different (up to 8%). By contrast, the traditional edge-MTFs lead to a highly different result (up to 40%) from the point-MTFs across all variations of spatial resolution.

3.2 Slanted Angle Variation

The point-MTF, traditional edge-MTF, and statistical edge-MTF curves at various slanted angles are shown in Figure 4, and their values of MTF 10% are tabulated in Table 2. The images were all blurred by 1 pixel. The statistical edge-MTF yielded similar results to the traditional edge-MTF. At a slanted angle of 0 - 8°, the statistical edge-MTF approach was comparable (to within about 2%) to the point-MTF. For slanted angles of 9° and above, the difference is up to 5% compared to the point-MTF. As expected, the traditional edge-MTF produces larger differences as the angle of the slanted edge increases. At an angle of 5° and above, the difference is more than 50%.

Accurate MTF measurement is essential to establish an accurate diagnosis. The study of Hata *et al*. [36] reported that a decrease in spatial resolution leads to a reduction of lesion detection qualitatively in eleven cadaver lung images. Besides point-MTF, edge-MTF is currently widely used for measuring spatial resolution of the image. The advantage of the edge-MTF is that it can be performed on any phantom, without the need for a special phantom, because any edge of any phantom can be used. The edge-MTF can produce more spread profiles compared to the point-MTF (where the number of profiles is limited) so that fluctuations in pixel values due to image noise can be minimized. Another advantage is that edge-MTF measurements can be carried out on objects with different contrast-to-noise ratio (CNR) values. This eventually led to the introduction of the task transfer function (TTF) concept which became very important in the era of iterative reconstruction (IR) and deep learning image reconstruction (DLIR). However, edge-MTF has its own challenges, including the need for accurate shifting of the ESF and it is more sensitive to noise due to the differentiation process from ESF to PSF.

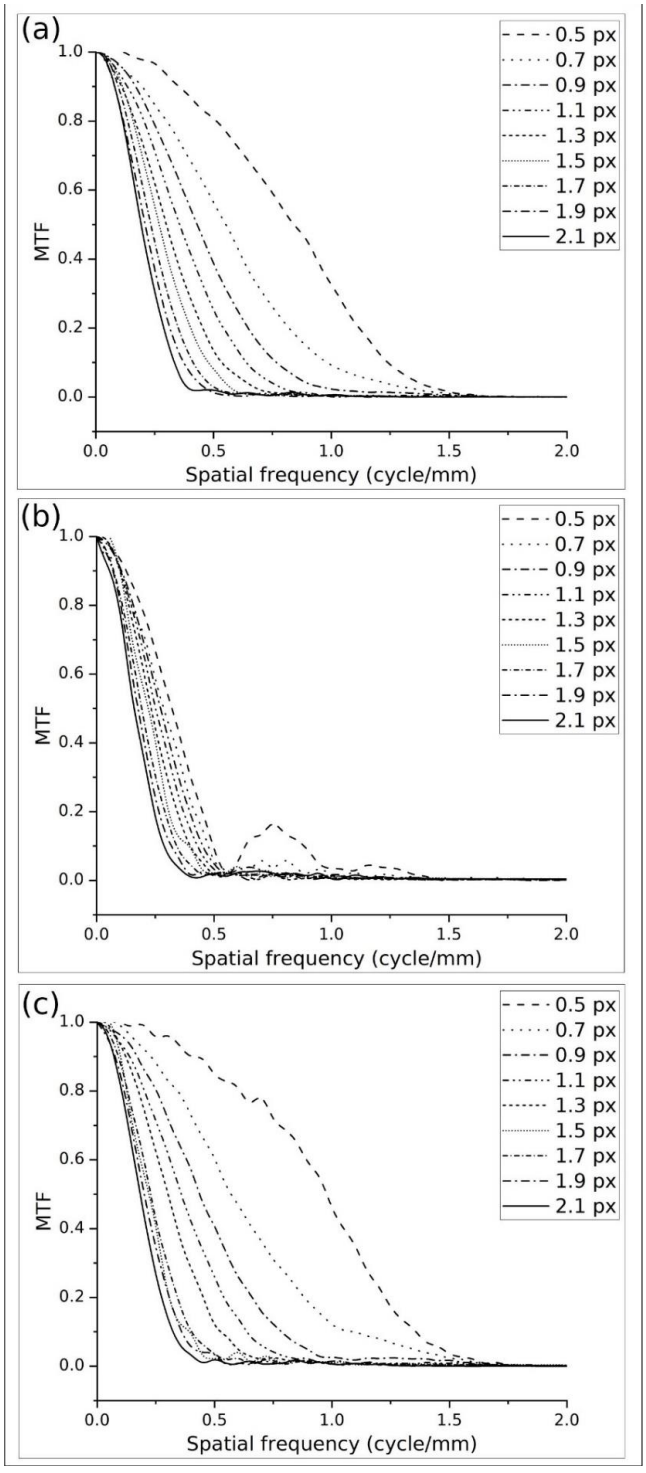

Figure 3 The MTF curves at various spatial resolutions from the three methods with various spatial resolutions (a) point-MTF, (b) traditional edge-MTF, and (c) statistical edge-MTF. The angle of the slanted image is 5°

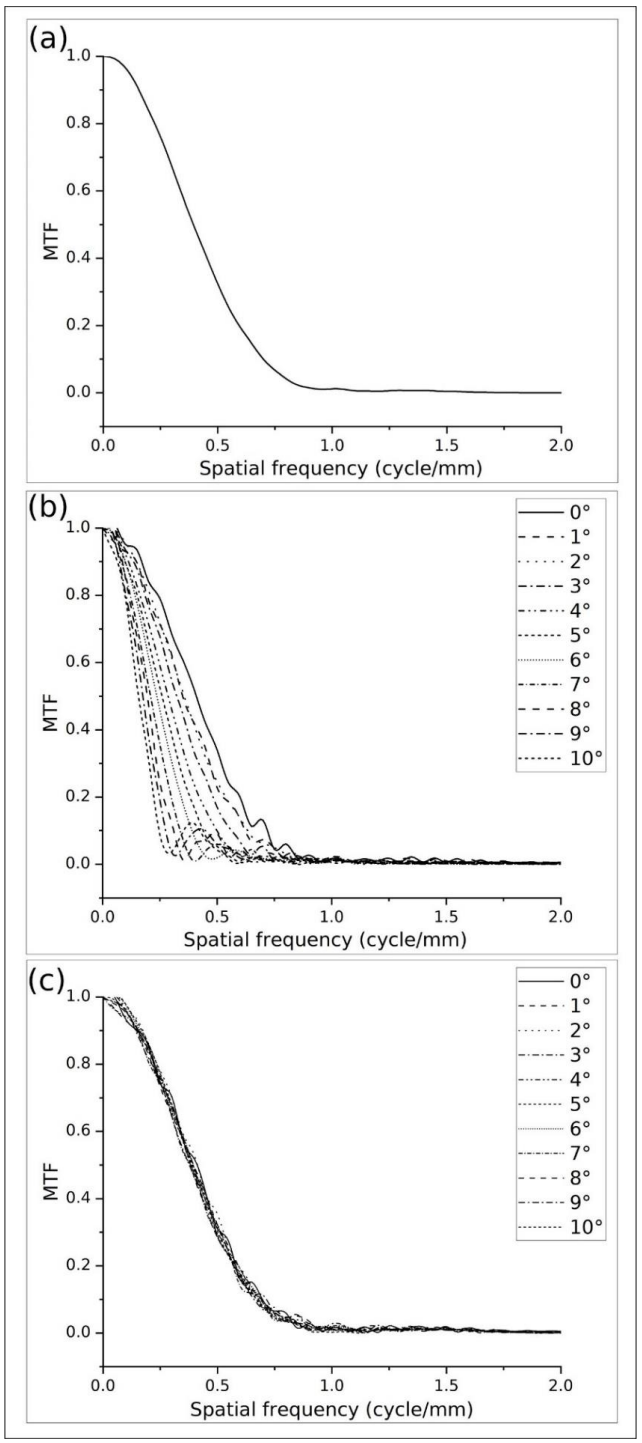

Figure 4 The MTF curves from three methods (a) point-MTF, (b) traditional edge-MTF at various slanted angles, and (c) statistical edge-MTF at various slanted angles. The images were blurred by 1 pixel

In the current study, the point-MTF is used as the gold standard, even though the point-MTF has its own limitations. Apart from producing a very limited number of profiles, its other limitations are that it is very dependent on the size of the ROI, it depends on the direction of the average (whether x-axis, y-axis, or polar direction), and it depends on the point position within the image. In this study, the point-MTF is calculated by averaging the x-axis direction. The point-MTF value is of course independent of the edge-angle.

The accurate shifting of ESF is essential for ensuring the accuracy of edge-MTF measurements using the edges of CT images. Many researchers [30-33] have studied this issue and have proposed various innovations to produce accurate edge-MTF curves. Unfortunately, these previous methods usually mandate that the position of edges must be exactly known, which is often difficult to achieve [13]. This study proposes an easier and faster approach to produce accurate ESF curves and obtain accurate edge-MTF curves. The current study used a statistical approach to assess the level of similarity between the shifted ESF and the reference ESF.

The statistical approach has been to be more resistant to errors in measuring the edge-MTF for different angles of the slanted objects compared to the traditional edge-MTF. The statistical shifting approach produced accurate edge-MTFs up to a slant of 0 - 8° (i.e., with a difference of around 2% from the point-MTF based on the 10% MTF values). At slant angles of 9° and more, the MTF 10% of the statistical approach produced a larger difference up to 5% from the point-MTF measurements. By contrast, the traditional edge-MTF led to very large differences (more than 50% at angles of 5° and above) compared to the point-MTF.

In the current study, the ESF shift was only 10 pixels forward and 10 pixels backward. At large slant angles, a shift of 10 pixels may be too small. Thus, to anticipate large slant angles in an object, the ESF shift can be increased, for example, to 20 pixels. However, this will increase computation time

The advantage of the statistical edge-MTF method is that it can be applied to irregular objects, for example to anthropomorphic phantoms or to clinical patient images. This opens a wider potential to measuring MTF in clinical images of patients, which still faces many challenges to date. However, evaluation on irregular surfaces has not been carried out in this study.

This proposed method has shortcomings, because this method does not accommodate the re-binning technique. Thus, this methodology is limited by the Nyquist theorem. For images with a FOV of 250 mm, the Nyquist frequency is 1.024 cycles/mm. This value is of course very small and cannot be used for CT images having high spatial resolution where values can exceed 1.5 cycles/mm. In the future, the statistical edge-MTF methodology will be extended to include binning techniques so that the Nyquist frequency can be increased several times.

Table 1 Values of MTF 10% resulting from the three methods of point-MTF, traditional edge-MTF, and statistical edge-MTF at various spatial resolutions. The angle of the slanted image is 5°

Blurring (px)	MTF 10% (cycle/mm)			Difference[a]		Difference[b]	
	Point	Traditional edge	Statistical edge	Percentage (%)	*p-value*	Percentage (%)	*p-value*
0.5	1.24 ± 0.00	0.77 ± 0.10	1.35 ± 0.01	37.90	0.00	8.87	0.00
0.7	1.01 ± 0.01	0.48 ± 0.01	1.07 ± 0.01	52.48	0.00	5.94	0.00
0.9	0.76 ± 0.01	0.46 ± 0.02	0.77 ± 0.02	40.05	0.00	0.78	0.51
1.1	0.64 ± 0.00	0.43 ± 0.01	0.65 ± 0.02	32.19	0.00	0.93	0.54
1.3	0.54 ± 0.00	0.39 ± 0.01	0.54 ± 0.01	27.51	0.00	0.37	0.77
1.5	0.47 ± 0.00	0.37 ± 0.01	0.47 ± 0.01	21.27	0.00	0.00	0.61
1.7	0.42 ± 0.00	0.34 ± 0.01	0.41 ± 0.00	17.70	0.00	1.91	0.00
1.9	0.37 ± 0.01	0.32 ± 0.00	0.37 ± 0.01	13.51	0.00	0.00	0.47
2.1	0.34 ± 0.00	0.30 ± 0.01	0.32 ± 0.00	11.76	0.00	5.88	0.00

[a] the difference between the point-MTF and the traditional edge-MTF

[b] the difference between the point-MTF and the statistical edge-MTF

Table 2 Values of MTF 10% resulting from the three methods of point-MTF, traditional edge-MTF, and statistical edge-MTF at various angles of slanted edge. Angle of slanted image is 5 degrees

Slanted Angle (°)	MTF 10% (cycle/mm)			Difference[a]		Difference[b]	
	Point	Traditional edge	Statistical edge	Percentage (%)	*p-value*	Percentage (%)	*p-value*
0	0.70 ± 0.01	0.69 ± 0.01	0.70 ± 0.01	1.17	0.18	1.71	0.65
1	0.70 ± 0.01	0.62 ± 0.02	0.70 ± 0.01	12.48	0.00	1.45	0.64
2	0.70 ± 0.01	0.63 ± 0.01	0.69 ± 0.01	11.18	0.00	1.59	0.22
3	0.70 ± 0.01	0.58 ± 0.01	0.69 ± 0.00	20.61	0.00	1.61	0.07
4	0.70 ± 0.01	0.50 ± 0.01	0.69 ± 0.00	38.07	0.00	1.01	0.28
5	0.70 ± 0.01	0.44 ± 0.01	0.69 ± 0.01	75.63	0.00	1.89	0.05
6	0.70 ± 0.01	0.39 ± 0.01	0.69 ± 0.01	57.02	0.00	2.05	0.00
7	0.70 ± 0.01	0.34 ± 0.01	0.68 ± 0.01	103.29	0.00	2.06	0.00
8	0.70 ± 0.01	0.30 ± 0.00	0.68 ± 0.01	132.33	0.00	2.07	0.00
9	0.70 ± 0.01	0.34 ± 0.03	0.67 ± 0.01	105.68	0.00	3.46	0.00
10	0.70 ± 0.01	0.38 ± 0.02	0.66 ± 0.01	84.94	0.00	5.17	0.00

[a] the difference between the point-MTF and the traditional edge-MTF

[b] the difference between the point-MTF and the statistical edge-MTF

This study has other limitations. The approach has only been tested on one type of phantom, i.e., a computational phantom. Testing on commonly used physical phantoms is necessary to investigate the algorithm's robustness against actual imaging conditions. Furthermore, the MTF measurements in this study only used one particular software, namely IndoQCT. Comparison with other software, such as iQmetrix and ImQuest, should be performed in further studies to test the method's robustness.

4.0 CONCLUSION

The statistical edge-MTF measurements produced spatial resolutions comparable to the point-MTF. Statistical edge-MTF can work well without knowing the edge pattern. At slant angles up to 8°, the statistical edge-MTF is within about 2% of the point-MTF. At larger angles, the difference from the point-MTF is greater. Statistical edge-MTF opens the way to edge-MTF measurements on irregular edges so that MTF measurements on clinical images can be more easily performed.

Acknowledgements

This work was funded by the World Class Research University (WCRU), Diponegoro University, No. 357-17/UN7.2/PP/IV/2024.

Conflicts of Interest

The author(s) declare(s) that there is no conflict of interest regarding the publication of this paper.

References

[1] Seeram Euclid. 2016. Chapter 12: Other Technical Applications of Computed Tomography Imaging. In *Computed Tomography: Physical Principles, Clinical Applications, and Quality Control*. 4th ed. USA: Elsevier.

[2] Morin, R. L., and Mahesh, M. 2018. The Importance of Spatial Resolution to Medical Imaging. *Journal of the American College of* Radiology. 15(8): 1127.

[3] Wikberg, E., van Essen, M., Rydén, T., Svensson, J., Gjertsson, P., Bernhardt, P. 2021. Evaluation of the Spatial Resolution in Monte Carlo-Based SPECT/CT Reconstruction of 111in-Octreotide Images. *Radiation Protection Dosimetry*. 195(3–4): 319–326.

[4] Rajendran, K., Petersilka, M., Henning, A., Shanblatt, E., Marsh, J., Jr, Thorne, J., Schmidt, B., Flohr, T., Fletcher, J., McCollough, C., Leng, S. 2021. Full Field-of-view, High-resolution, Photon-counting Detector CT: Technical Assessment and Initial Patient Experience. *Physics in Medicine and Biology*. 66(20). 10.1088/1361-6560/ac155e.

[5] Sugisawa, K., Ichikawa, K., Urikura, A., Minamishima, K., Masuda, S., Hoshino, T., Nakahara, A., Yamada, Y., Jinzaki, M. 2020. Spatial Resolution Compensation by Adjusting the Reconstruction Kernels for Iterative Reconstruction Images of Computed Tomography. *Physica Medica.* 74: 47–55.

[6] Rossmann, K. 1969. Point Spread-function, Line Spread-function, and Modulation Transfer Function. Tools for the Study of Imaging Systems. *Radiology*. 93(2): 257–272.

[7] Wu, P., Boone, J. M., Hernandez, A. M., Mahesh, M., Siewerdsen, J. H. 2021. Theory, Method, and Test Tools for Determination of 3D MTF Characteristics in Cone-beam CT. *Medical Physics*. 48(6): 2772–2789.

[8] Kayugawa, A., Ohkubo, M., Wada, S. 2013. Accurate Determination of CT Point-spread-function with High Precision. *Journal of Applied Clinical Medical Physics*. 14(4): 3905.

[9] Boone, J. M., and Seibert, J. A. 1994. An Analytical Edge Spread Function Model for Computer Fitting and Subsequent Calculation of the LSF and MTF. *Medical Physics*. 21(10): 1541–1545

[10] Fountos, G. P., Michail, C. M., Zanglis, A., Samartzis, A., Martini, N., Koukou, V., Kalatzis, I., Kandarakis, I. S. 2012. A Novel Easy-to-use Phantom for the Determination of MTF in SPECT Scanners. *Medical Physics*. 39(3):1561–1570.

[11] Harms, A. A., and Zeilinger, A. 1977. A New Formulation of Total Unsharpness in Radiography. *Physics in Medicine & Biology*. 22(1): 70–80.

[12] Spiegler, P., and Norman, A. 1973. The Total Unsharpness in Radiography. *Physics in Medicine & Biology*. 18(6): 884–887.

[13] Xie, X., Fan, H., Wang, A., Zou, N., Zhang, Y. 2018. Regularized Slanted-edge Method for Measuring the Modulation Transfer Function of Imaging Systems. *Applied Optics*. 57(22): 6552–6558.

[14] Friedman, S. N., and Cunningham, I. A. 2008. A Moving Slanted-edge Method to Measure the Temporal Modulation Transfer Function of Fluoroscopic Systems. *Medical Physics*. 35(6): 2473–2484.

[15] Masaoka, K., Yamashita, T., Nishida, Y., Sugawara, M. 2014. Modified Slanted-edge Method and Multidirectional Modulation Transfer Function Estimation. *Optics Express*. 22(5): 6040–6046.

[16] Zhang, S., Wang, F., Wu, X., Gao, K. 2023. MTF Measurement by Slanted-edge Method Based on Improved Zernike Moments. *Sensors (Basel)*. 23(1): 509.

[17] Boone, J. M. 2001. Determination of the Presampled MTF in Computed Tomography. *Medical Physics*. 28(3): 356–360.

[18] Kawagishi, N., R. Kakinuma, H. Yamamoto. 2020. Aerial Image Resolution Measurement based on the Slanted Knife Edge Method. *Optics Express*. 28(24): 35518–35527

[19] Zhou, Z., Gao, F., Zhao, H., Zhang, L., Ren, L., Li, Z., Ghani, M. U., Hao, T., Liu, H. 2015. Improving the Accuracy of MTF Measurement at Low Frequencies based on Oversampled Edge Spread Function Deconvolution. *Journal of X-ray Science and Technology*. 23(4): 517–529.

[20] Nishi, K. 2023. Does the Slanted-edge Method Provide the True Value of Spatial Frequency response? *Journal of the Optical Society of America. A, Optics, Image Science, and Vision*. 40(2): 259–269.

[21] Zhou, Z., Zhu, Q., Zhao, H., Zhang, L., Ma, W., Gao, F. 2014. Techniques to Improve the Accuracy of Presampling MTF Measurement in Digital X-ray Imaging based on Constrained Spline Regression. *IEEE Transactions on Biomedical Engineering*. 61(4): 1339–1349.

[22] Samei, E., Buhr, E., Granfors, P., Vandenbroucke, D., Wang, X. 2005. Comparison of Edge Analysis Techniques for the Determination of the MTF of Digital Radiographic Systems. *Physics in Medicine and Biology*. 50(15): 3613–3625.

[23] Yuan, H., Guo, Y., Si, G., Li, Y., Qu, L. 2015. MTF Measurement Method Based on Slanted-Edge Image Simulated by Normal Distribution. *Acta Optica Sinica*. 35(7): 172–181.

[24] Mori, I., and Machida, Y. 2009. Deriving the Modulation Transfer Function of CT from Extremely Noisy Edge Profiles. *Radiological Physics and Technology*. 2(1): 22–32.

[25] Anam, C., Sutanto, H., Adi, K., Budi, W. S., Muhlisin, Z., Haryanto, F., Matsubara, K., Fujibuchi, T., Dougherty, G. 2020. Development of a Computational Phantom for Validation of Automated Noise Measurement in CT Images. *Biomedical Physics and Engineering Express*. 6(6). 10.1088/2057-1976/abb2f8.

[26] Anam, C., Triadyaksa, P., Naufal, A., Arifin, Z., Muhlisin, Z., Setiawati, E., Budi, W. S. 2022. Impact of ROI Size on the Accuracy of Noise Measurement in CT on Computational and ACR Phantoms. *Journal of Biomedical Physics and Engineering*. 12(4): 359–368.

[27] Anam, C., Amilia, R., Naufal, A., Sutanto, H., Dwihapsari, Y., Fujibuchi, T., Dougherty, G. 2023. Impact of Noise Level on the Accuracy of Automated Measurement of CT Number Linearity on ACR CT and Computational Phantoms *Journal of Biomedical Physics and Engineering*. 13(4): 353–362.

[28] Anam, C., Fujibuchi, T., Haryanto, F., Budi, W.S., Sutanto, H., Adi, K., Muhlisin, Z., Dougherty, G. 2019. Automated MTF Measurement in CT Images with a Simple Wire Phantom. *Polish Journal of Medical Physics and Engineering*. 25(3): 179–187.

[29] Anam, C., Fujibuchi, T., Budi, W. S., Haryanto, F., Dougherty, G. 2018. An Algorithm for Automated Modulation Transfer Function Measurement using an Edge of a PMMA Phantom: Impact of Field of View on Spatial Resolution of CT Images. *Journal of Applied Clinical Medical Physics*. 19(6): 244–252.

[30] Buhr, E., Günther-Kohfahl, S., Neitzel, U. 2003. Accuracy of a Simple Method for Deriving the Presampled Modulation Transfer Function of a Digital Radiographic System from an Edge Image. *Medical Physics*. 30(9): 2323–2331.